Available online at www.sciencedirect.com
SCIENCE DIRECT®
International Journal of Mass Spectrometry 231 (2004) 83–95
International Journal of Mass Spectrometry
www.elsevier.com/locate/ijms

Catalyzed isomerization and decarbonylation of ionized formic acid and dihydroxycarbene

Guillaume van der Rest*, Philippe Mourgues, Henri E. Audier

Laboratoire des Mécanismes Réactionnels, CNRS UMR 7651, École Polytechnique, 91128 Palaiseau Cedex, France

Received 8 January 2003; accepted 7 October 2003

This work is dedicated to Helmut Schwarz for his 60th birthday.

Abstract

Catalyzed conversion of $HCOOH^{\bullet+}$ into $HOCOH^{\bullet+}$ was studied in the cell of a FT-ICR in the presence of different molecules. The reaction of $HCOOH^{\bullet+}$ with SO_2, whose proton affinity (PA) lies between that of the $HOCO^{\bullet}$ radical at the carbon and at the oxygen sites, yields the $HOCOH^{\bullet+}$ carbene isomer as proved by its characteristic reaction with cyclopropane. When the PA of the catalyst lies above the highest PA of both sites of the $HOCO^{\bullet}$ radical, formation of $HOCOH^{\bullet+}$ cannot be observed since its final state lies above that corresponding to protonation of the catalyst. However, reactions of $DCO_2H^{\bullet+}$ and of $HCO_2D^{\bullet+}$, which protonate several catalysts in an identical ratio which is very near of 1/1 at the beginning of the reaction, indicates that both ions, $DCO_2H^{\bullet+}$ and of $HCO_2D^{\bullet+}$, convert into ion DO-C-$OH^{\bullet+}$ within a complex prior to protonation. The reactions of $HCOOH^{\bullet+}$ and $HOCOH^{\bullet+}$ with water were also more particularly studied by using theoretical calculations. Both reactions lead to protonated water and to the ionized water dimer which has been shown to possess the $[H_2OH^+\cdots OH^{\bullet}]$ structure. The first step of the process is the conversion of the $[HO(O)C^{\bullet}\cdots H^+\cdots OH_2]$ complex into $[HOCO^{\bullet}\cdots H^+\cdots OH_2]$. This latter complex undergoes two main pathways: on the one hand, it leads to protonation of water; on the other hand, it isomerizes to the $[O^{\bullet}COH\cdots H^+\cdots OH_2]$ intermediate which dissociates to form $[H_2OH^+\cdots OH^{\bullet}]$ with CO loss. Formation of H_3O^+ and $[H_2OH^+\cdots OH^{\bullet}]$ being rapid, the $[HOCO^{\bullet}\cdots H^+\cdots OH_2]$ complex does not dissociate to yield the ionized carbene product which was not detected. Since the catalyzed isomerization of the 1,2-H transfer, converting $HCOOH^{\bullet+}$ into $HOCOH^{\bullet+}$, is only observed within the corresponding complexes, this is a typical case of hidden isomerization. Finally, the differences in the unimolecular fragmentations of ionized formic acid and of its water solvated ion were explained.

Keywords: Catalyzed isomerizations; Ionized dihydroxycarbenes; Ionized formic acid; FT-ICR mass spectrometry; Ab initio calculations

1. Introduction

In the gas phase, intramolecular $H^{\bullet}$ transfer in radical cations is a well known process which can occur both to an ionized heteroatom radical or to a radical carbon site. These two kinds of $H^{\bullet}$ transfer were extensively studied by Helmut Schwarz [1] in several systems, more particularly in alkanoic acid radical cations.

Intramolecular $H^{\bullet}$ transfer to the heteroatom is often the first step of the fragmentation of long-chain alcohols, ethers, amines, acids or esters radical cations. Such a process yields a distonic ion [2–4]. Experiments show that intramolecular 1,2-$H^{\bullet}$ transfers to an ionized heteroatom are generally not observed (see for example [5]), 1,3-$H^{\bullet}$ transfers are rare and irreversible [6], while 1,4, and a fortiori 1,5 and 1,6-$H^{\bullet}$ transfers are easier and often reversible. This has been confirmed by calculations carried out on ionized amines [7] as well as on ionized alcohols [8]. Therefore, 1,2 and 1,3-hydrogen transfers in radical cations, and more rarely in cations, are the rate limiting steps inhibiting isomerization reactions of ions. However, such processes can be catalyzed by appropriate neutral molecules. This has been reviewed by different authors [9–11].

1,2-H "transport" reactions were first demonstrated in small systems involving a cation Eq. (1) or radical cations Eq. (2) [9]. A second group of catalyzed isomerizations concerns the interconversion between molecular ions and their α-distonic counterparts Eq. (3). These studies involve a great number of experimental methods as well as calculations on different systems [12,13]. Finally, a third group of reactions

* Corresponding author.
E-mail address: gvdr@dcmr.polytechnique.fr (G.v.d. Rest).

1387-3806/$ – see front matter © 2003 Elsevier B.V. All rights reserved.
doi:10.1016/j.ijms.2003.10.001

more recently studied, corresponds to the interconversion between molecular ions and their ionized carbene isomers [14,15].

$$COH^+ \rightarrow CHO^+ \quad (1)$$

$$HCN^{\bullet+} \rightarrow CNH^{\bullet+} \quad (2)$$

$$CH_3OH^{\bullet+} \rightarrow {}^{\bullet}CH_2OH_2{}^+ \quad (3)$$

The first 1,3-H transport, conversion of ionized 2,4-cyclohexadienone into ionized phenol catalyzed by water, has been proposed by Helmut Schwarz [1a]. More generally, a number of works deals with the mechanism of keto-enol tautomerism in ions [16].

Finally, we have recently shown that only one molecule of solvent can catalyze successive 1,2-H and 1,3-H transfers. For instance, water catalyzes all the steps of the decarbonylation of ionized formamide [14] Eq. (4) and more particularly its conversion into the ionized carbene NH_2-C-$OH^{\bullet+}$.

$$[H_2N{-}CH{=}O^{\bullet+}, H_2O] \overset{1,2\text{-H}}{\rightarrow} [H_2N\text{-}C\text{-}OH^{\bullet+}, H_2O] \overset{1,3\text{-H}}{\rightarrow} [H_2O\cdots H_3N{-}C{=}O^{\bullet+}] \rightarrow [NH_3, H_2O]^{\bullet+} + CO \quad (4)$$

The first goal of this work is to study the catalysts which operate in the conversion of formic acid **FA**$^{\bullet+}$ into the dihydroxycarbene **HyC**$^{\bullet+}$ radical cation. The second goal is to show that water catalyzes also the decarbonylation of **FA**$^{\bullet+}$.

Metastable **FA**$^{\bullet+}$ and **HyC**$^{\bullet+}$ lead dominantly to a hydrogen radical loss, but elimination of a hydroxy radical as well as that of CO giving ionized water, are also observed to some extent [17]. Helmut Schwarz has shown that these fragmentations involve high energy barriers [18].

As already pointed out by Hrùsak et al. [19], and as is the case for a number of carbene ions [14,15], there is no covalent addition of the water molecule to the HO–C–$OH^{\bullet+}$ carbene, the only stable structures are H-bonded ones. In this work, it will be shown that water catalyzes the decarbonylation of ionized formic acid and of ionized dihydroxycarbene. It will be also explained why the unimolecular reactions of the bare and solvated ions are significantly different.

2. Methods

2.1. Experimental

The bimolecular reactions of ions were examined in a Bruker CMS-47X FT-ICR mass spectrometer equipped with an external ion source and an infinity cell [20]. Water was introduced into the cell by means of a leak valve at a static pressure of 1×10^{-8} and then diluted in an argon gas bath to a total pressure of 2×10^{-7} mbar. When appropriate, other neutral reactants were introduced by means of a solenoid pulsed valve at peak pressures in the 10^{-6} mbar range.

Ion-molecule reactions were examined after isolation and thermalization of the reactant ions formed in the external source. After transfer into the cell, the ions of interest were first isolated by radio frequency ejection of all unwanted ions. After a 1.5 s delay to allow thermalization of the ions by successive collisions with argon, the isolation procedure was repeated by the use of low-voltage single frequency pulses (soft shots) at the resonance frequencies of the product ions formed during the relaxation time. Reaction time was varied, and the intensity ratio of each peak over the total intensity leads to kinetic data. Reaction efficiencies (Eff) are expressed as the ratio (expressed in %) of the experimental rate constant over the collision rate constant calculated according to Su and Chesnavich [21]. Errors on experimental values are estimated at ±30%.

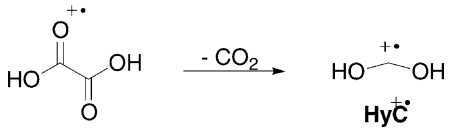

Scheme 1.

Ionized formic acid (FA$^{\bullet+}$) was produced by direct electron ionization (EI) of neutral formic acid. Ionized dihydroxycarbene HOCOH$^{\bullet+}$ (HyC$^{\bullet+}$) was produced by fragmentation of the molecular ion of oxalic acid as described elsewhere (Scheme 1) [22]. Most reagents were commercially available and used without further purification. For introduction in the leak and pulsed valves, the liquid reagents were subject to several freeze-pump-thaw cycles. D-labeled formic acid (HCOOD) was produced by the direct mixture of HCOOH with a large excess of D_2O in the introduction reservoir of the external source. Exclusive selection of the *m*/*z* 47 ion (HCOOD$^{\bullet+}$) provided the purification step of the labeled compound. DCO_2H and $H_2{}^{18}O$ (95% ^{18}O) are commercially available.

2.2. Calculations

The Gaussian 98 program package [23] was used to determine geometries and energies of the different structures. The geometries were optimized at the UMP2/6-31G** level of the theory unless stated otherwise. Diagonalization of the computed Hessian matrix was performed in order to confirm that the structures were either minima or transition states on the potential energy surface. Zero point energies and thermal energies at 298.15 K were computed at this level of the theory and scaled by a 0.93 factor [24]. To improve the accuracy in the energy determination and account for basis set and electron correlation effects, further single-point calculations were performed following the G3(MP2) method [25].

3. Experimental results

The first goal of this work is to study the catalyzed conversion of formic acid **FA**$^{\bullet+}$, into its dihydroxycarbene isomer **HyC**$^{\bullet+}$. For this purpose, the reactions with molecules

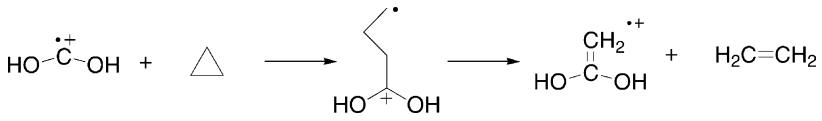

Scheme 2.

possessing different PA were performed. The second goal being the study of the water catalyzed decarbonylation of these ions, detailed experiments and calculations were carried out in order to determine the mechanism of the reactions observed.

3.1. Reaction of $FA^{\bullet+}$ with CO

In the presence of CO (PA = 142 kcal mol^{-1}), $\mathbf{FA}^{\bullet+}$ only leads to a slow isomerization into $\mathbf{HyC}^{\bullet+}$. After one second of reaction (CO pressure = 10^{-7} mbar), this latter ion was detected by its reactions with cyclopropane. The dominant process (90%) corresponds to the protonation of cyclopropane, but for 10% a $C_2O_2H_4^{\bullet+}$ product is formed, corresponding to the characteristic reaction of the carbene structure [15] (Scheme 2). In the same conditions (CO pressure = 10^{-7} mbar), the direct reaction of $\mathbf{HyC}^{\bullet+}$ with cyclopropane yields the same products in the same branching ratio, indicating that in the conditions described above, the conversion of $\mathbf{FA}^{\bullet+}$ into $\mathbf{HyC}^{\bullet+}$ is almost complete.

3.2. Reactions with CH_3Cl and CS_2

With CH_3Cl (PA = 154.7 kcal mol^{-1}, ionization energy (IE) = 11.22 eV)[26], the main reaction of $\mathbf{FA}^{\bullet+}$ (IE(**FA**) = 11.33 eV) is, as expected, electron transfer and subsequent self-chemical ionization of CH_3Cl. This has for consequence a very low yield of isomerization. Similarly, CS_2 (PA = 163 kcal mol^{-1}, IE = 10.07 eV), whose ionization energy lies about one eV below that of formic acid [26a], only leads to electron transfer. After reisolation of $\mathbf{FA}^{\bullet+}$, the characteristic reaction of $\mathbf{HyC}^{\bullet+}$ with a pulse of cyclopropane (Scheme 2) is not observed.

3.3. Reactions with SO_2

With SO_2 (PA = 160.7 kcal mol^{-1}, IE = 12.32 eV) [26], both studied ions, $\mathbf{FA}^{\bullet+}$ and $\mathbf{HyC}^{\bullet+}$, yield the same reactions at the same rate (Eff = 20%), which suggests that these ions interconvert prior to dissociation. The main reaction is the loss of CO_2 from the encounter complex to yield presumably the $HOSOH^{\bullet+}$ product (ionized sulfinic acid) which has been recently described by other authors [27]. Reaction of $DCOOH^{\bullet+}$ yields $DOSOH^{\bullet+}$. The mechanism of this interesting process will be discussed elsewhere. $\mathbf{FA}^{\bullet+}$ undergoes a second reaction, namely an isomerization. Indeed, after collision with SO_2, $\mathbf{FA}^{\bullet+}$ converts into $\mathbf{HyC}^{\bullet+}$, since the so formed ion reacts, in turn, with a pulse of cyclopropane both by protonation of the neutral and by formation of the $C_2O_2H_4^{\bullet+}$ product (Scheme 2). Similarly, $DCOOH^{\bullet+}$ is converted into $DOCOH^{\bullet+}$, since cyclopropane is deuteronated in a 1/1 ratio while a $C_2O_2H_3D^{\bullet+}$ product is formed.

3.4. Reactions with H_2O

3.4.1. Products of the reactions

Ionized formic acid ($\mathbf{FA}^{\bullet+}$) and ionized dihydroxycarbene ($\mathbf{HyC}^{\bullet+}$) both react with water in a similar way at near collision rate (Eff = 99% for $\mathbf{FA}^{\bullet+}$, 89% for $\mathbf{HyC}^{\bullet+}$). Only two primary product ions are observed: a major ion *m/z* 19 (H_3O^+) and a minor ion *m/z* 36 ($H_4O_2^{\bullet+}$) (Fig. 1). This latter, which is formally an ionized water dimer, evolves by further reaction with water at unit efficiency, leading to the *m/z* 37 ion ($H_5O_2^+$), as shown by reselection and further reaction of the *m/z* 36 ion. This *m/z* 37 ion is not formed by the simple reaction of ionized water $H_2O^{\bullet+}$ or protonated water H_3O^+ with water in the FT-ICR cell in our pressure conditions. Worth to note, continuous fast ejection of the water dimer radical cation does not reduce significantly the amount of protonated water, which means that formation of H_3O^+ occurs either mainly directly, or through water dimers complexes having a very short lifetime (ejection time 70 μs) [14].

The ionized water dimer has been studied in detail, both on experimental and theoretical grounds, by a number of groups [28–31]. The bimolecular reactions of this dimer have been extensively studied by Nibbering's group [31], and result in electron transfer, proton transfer and replacement of $OH^{\bullet}$ by the neutral reactant. It was calculated that two stable structures exist for the dimer: either a two center-three electron bound $[H_2O\cdots OH_2]^{\bullet+}$ symmetrical system or a hydrogen bound $[H_2OH^+\cdots OH^{\bullet}]$ system. The calculated relative energies for the dimers, the transition state between them and the two decomposition pathways are shown in Scheme 3. In Nibbering's experiments, it was assumed, on thermodynamical considerations, that the ionized dimer has the more stable structure, described as a H-bonded complex between H_3O^+ and $OH^{\bullet}$.

The collision induced dissociation (CID) spectra the water dimer formed by reaction of formic acid with water was performed. Upon collision, in contrast with the $[NH_3, H_2O]^{\bullet+}$ system [14] which yields only $NH_3^{\bullet+}$, the studied water dimer gives only H_3O^+, which is in agreement with the $[H_2OH^+\cdots OH^{\bullet}]$ structure. Conversely, this result is in coherence with the lack of substitution of a water molecule and with the exchange of a hydroxyl group since, in the case of the $[H_2OH^+\cdots OH^{\bullet}]$ structure, the much lower pro-

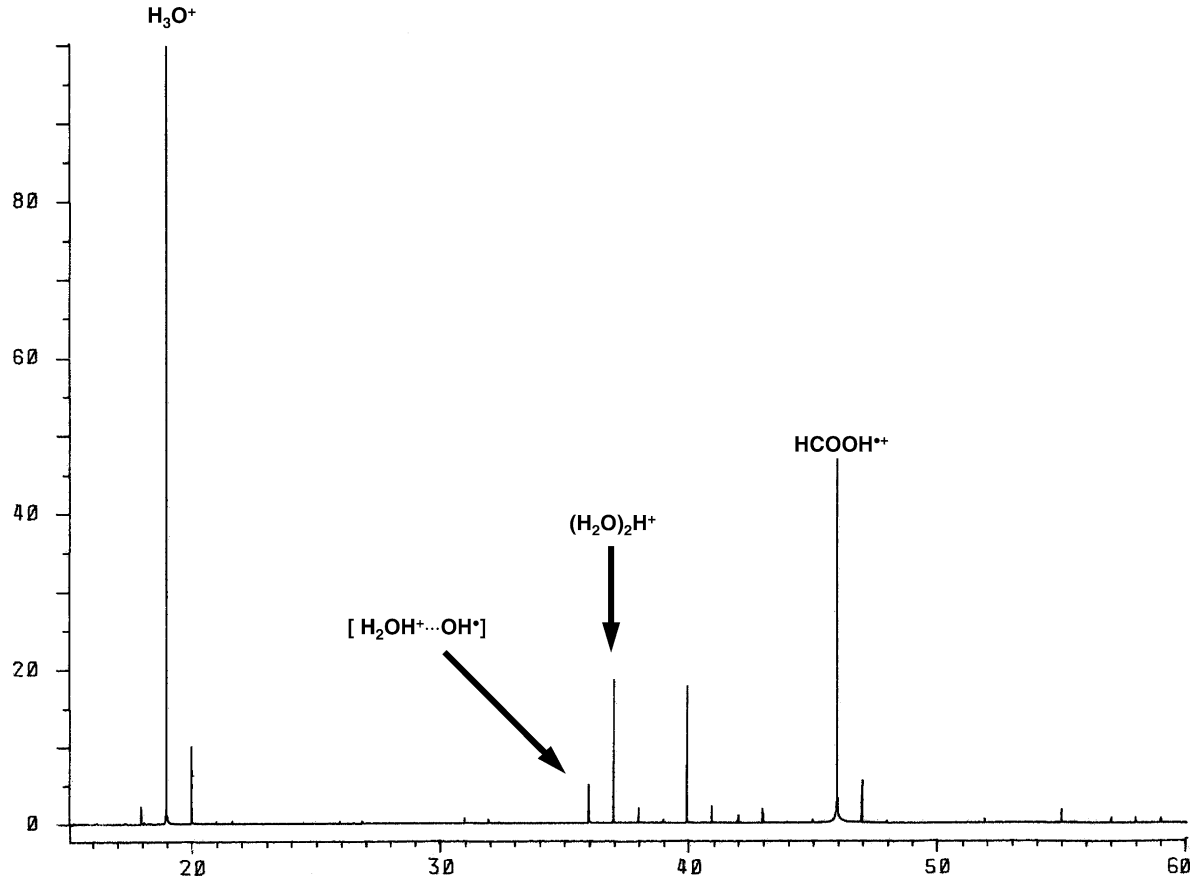

Fig. 1. Products of the reaction between $HCOOH^{\bullet+}$ and H_2O ($P = 1.2 \times 10^{-8}$ mbar) after 1.6 s reaction time.

ton affinity of $OH^{\bullet}$ (141.8 kcal mol^{-1}) [26b] compared to that of water (165.2 kcal mol^{-1}) suggests that formation of the proton bound dimer takes place via a ligand exchange, switching H_2O for $OH^{\bullet}$ Eq. (5).

$$[H_2OH^+ \cdots OH^{\bullet}] + H_2O \rightarrow [H_2O \cdots H^+ \cdots OH_2] + OH^{\bullet} \quad (5)$$

3.4.2. Reaction with $H_2{}^{18}O$

The reaction with oxygen labeled water could improve the determination of the structure of the water dimer radical cation: three oxygen atoms are involved in the intermediate [$HCOOH^{\bullet+}$, H_2O] or [$HOCOH^{\bullet+}$, H_2O] complexes. Two kinds of results can be expected. First, it is of interest to see whether the oxygen borne by the water molecule can be exchanged with either oxygen atoms of the radical cation before the loss of CO. Experiment indicates that a $[H_4O^{18}O]^{\bullet+}$ product is formed which means that the oxygen atom eliminated in the CO molecule comes exclusively from the reacting ion.

Second, after CO loss, the equivalence or not of the two oxygen atoms in the water dimer radical cation can give valuable information about its structure and about the mechanism of its formation. Since upon collision, the $[H_4O^{18}O]^{\bullet+}$ product only yields $H_3{}^{18}O^+$, it can be concluded that the symmetrical $[H_2O \cdots OH_2]^{\bullet+}$ two centers three electron bond structure is neither formed nor intermediate. Furthermore, the ion has a $[H_2{}^{18}OH^+ \cdots {}^{16}OH^{\bullet}]$ structure, where the oxonium moiety comes exclusively from the reacting water.

3.4.3. Reaction with D_2O

At low reaction times, the protonated water appears in a ratio *m/z* 20 (DH_2O^+)/*m/z* 21 (D_2HO^+) about 1/10, the purity of D_2O being taken into account. If the reaction was purely an exothermic proton transfer from the ionized carbene to the water molecule, no *m/z* 20 would have

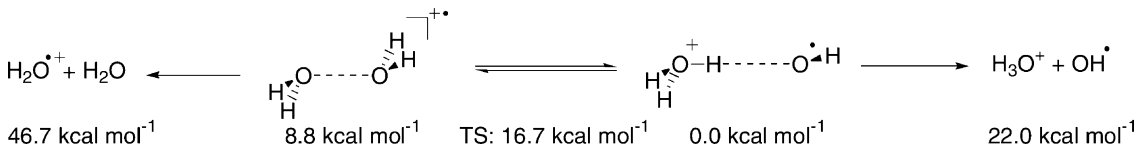

Scheme 3. Relative stability of the water dimers and decomposition pathways.

been observed. In agreement with this data, $DCO_2H^{\bullet+}$ and $HCO_2D^{\bullet+}$ protonate water in an identical ratio which is nearby 1/1 at the just beginning of the reaction. Therefore, in the protonation pathway, the H/D exchange is marginal which means that the intermediate complex does not exhibit a lifetime sufficient to undergo an extensive proton exchange.

Upon collision, the water dimer ion leads dominantly (about 75%) to a D_2HO^+ fragment corresponding therefore to the $[D_2OH^+ \cdots OH^{\bullet}]$ structure, DH_2O^+ accounting for the remaining 25%. These results indicate that there is only a partial H/D exchange prior to dissociation: a complete H/D scrambling would lead to a 1/1 ratio for the two fragment ions.

3.4.4. Subsequent reaction with cyclopropane

When the ion **FA**$^{\bullet+}$ is left in the cell in presence of water, reaction of this ion with a pulse of cyclopropane leads only to protonation, in contrast with the reactions observed with CO and SO_2. Therefore no intermediate formation of **HyC**$^{\bullet+}$ is observed, in line with the fact that the decarbonylation reaction occurs at collision rate. No back dissociation of the encounter complex [**FA**$^{\bullet+}$, H_2O] into **HyC**$^{\bullet+} + H_2O$, is observed. A similar behaviour was noticed for the reaction of $CH_3OH^{+\bullet}$ with CH_3OH [12].

3.5. Reaction with CH_2O

Three reaction channels, in a respective 2/1/1 ratio, are observed when formaldehyde (PA = 170.4 kcal mol^{-1}, IE = 10.87 eV) [26] reacts with **FA**$^{\bullet+}$: protonation of CH_2O, electron transfer and H$^{\bullet}$ abstraction. When DCOOH is used as reactant, protonation by H^+ and by D^+ are observed in a 1/1 ratio at the beginning of the reaction.

4. Discussion

4.1. Isomerized products and hidden isomerization

4.1.1. Previous studies on hidden catalyzed isomerizations

A number of experimental and theoretical studies deals with the catalyzed interconversion between a molecular ion $CH_3X^{\bullet+}$ (X = OH, OCH_3, SH, NH_2, etc.) and its α-distonic counterpart $^{\bullet}CH_2XH^+$. In all these isomerizations, the less stable isomer is converted, using an appropriate catalyst, into the more stable one [12,13]. The efficiency of the catalyst has been discussed. It has been shown [12] that at least two factors are important. First, the catalyst must possess an appropriate ionization energy in order to avoid the electron transfer reaction. Second, taking as example the systems where the distonic ion is the most stable structure, the proton affinity of the catalyst must be high enough to abstract a proton at the carbon site of the $CH_3X^{\bullet+}$ ion, but not too high in order to give back this proton to the heteroatom site. More precisely, three cases can be distinguished:

(i) When the PA of the catalyst lies below that of the $CH_2X^{\bullet}$ radical at the carbon site, the isomerization is either slow or not observed.

(ii) When the PA lies between that of $CH_2X^{\bullet}$ radical at the carbon site and that at the heteroatom site, the isomerized $^{\bullet}CH_2XH^+$ ion is generally a product of the reaction. For instance in the water catalyzed conversion of ionized methanol Eq. (3), the $^{\bullet}CH_2OH_2^+$ product has been clearly characterized by its CID spectrum [12a].

(iii) When the PA lies above the highest PA of both sites of the $CH_2X^{\bullet}$ radical, the $[^{\bullet}CH_2XH^+ \cdots$ catalyst] has a very short lifetime and rapidly leads to the protonated catalyst as final product. This final state lies necessarily below that corresponding to the formation of $^{\bullet}CH_2XH^+$, which therefore is not formed. However, even when the isomerized ion is not detected, hidden isomerizations can take place within complexes, which can only be detected by labeling. For instance, it has been shown by labeling that protonation of neutral methanol by ionized methanol is preceded by the conversion of the ion into its distonic counterpart Eq. (6) [12]. When the reaction is performed by using $CD_3OH^{\bullet+}$, protonation takes place either by H^+ or by D^+ in a 1/1 ratio, indicating that the protonating agent is the α-distonic ion $^{\bullet}CH_2OHD^+$. Similarly, in the reaction of $CD_3NH_2^{\bullet+}$ with a molecule of appropriate PA, protonation of the neutral takes place either by H^+ or by D^+ in a 2/1 ratio, since the protonating agent is the α-distonic ion $^{\bullet}CH_2NH_2D^+$. In both cases, isomerization obviously occurs within the intermediate complex but the α-distonic ion is not detected as a final product [12].

$$\begin{aligned} &CH_3OH^{\bullet+} + CH_3OH \\ &\rightarrow [CH_3OH^{\bullet+}, CH_3OH] \rightarrow [^{\bullet}CH_2OH_2^+, CH_3OH] \\ &\rightarrow CH_3OH_2^+ + {}^{\bullet}CH_2OH \end{aligned} \quad (6)$$

4.1.2. The case of ionized formic acid

For ionized formic acid, calculations indicate that the PA of the $HOCO^{\bullet}$ radical is 162.0 kcal mol^{-1} at the oxygen site and 152.5 kcal mol^{-1} at the carbon site.

(i) The PA of CO (142.0 kcal mol^{-1}) is less than the PA of the $HOCO^{\bullet}$ radical at the carbon site. Therefore, the catalyzed isomerization of **FA**$^{\bullet+}$ into **HyC**$^{\bullet+}$ is slow.

(ii) Three molecules used as neutral reactant possess a PA which lies between (or close to) that of $HOCO^{\bullet}$ radical at the carbon site and at the heteroatom site: CH_3Cl (PA = 154.7 kcal mol^{-1}), CS_2 (PA = 163.0 kcal mol^{-1}) and SO_2 (PA = 160.7 kcal mol^{-1}). The two first compounds do not operate as a catalyst since they react by electron transfer. In contrast catalyzed formation of **HyC**$^{\bullet+}$ by SO_2 was clearly established by the reactions of $HCO_2H^{\bullet+}$ and of $DCO_2H^{\bullet+}$ with cyclopropane performed after some reaction time and reisolation.

(iii) The PA of water (PA = 165.2 kcal mol^{-1}) lies above the highest PA of both sites of the HOCO$^{\bullet}$ radical. Formation of **HyC**$^{\bullet+}$ cannot be observed since its final state lies above that corresponding to H_3O^+ formation. However, the formation of the same products by reaction of **FA**$^{\bullet+}$ and **HyC**$^{\bullet+}$ with water, with about the same ratio $H_3O^+/H_4O_2^{\bullet+}$, and at the same rate, strongly suggests that these ions interconvert within complexes. Furthermore, reactions of $DCO_2H^{\bullet+}$ and of $HCO_2D^{\bullet+}$ protonate water in an identical ratio which is very near to 1/1 at the very beginning of the reaction. This indicates that both ions, $DCO_2H^{\bullet+}$ and of $HCO_2D^{\bullet+}$, convert into DO–C–OH$^{\bullet+}$ prior to protonation.

Of course, it could be objected that, fortuitously, $DCO_2H^{\bullet+}$ and $HCO_2D^{\bullet+}$ protonate water by H^+ or D^+ in a 1/1 ratio via two different mechanisms. However, since the same 1/1 ratio is also observed when these ions protonate SO_2 (PA = 160.7 kcal mol^{-1}) as well as formaldehyde (PA = 170.4 kcal mol^{-1}), whose PA significantly differ from that of water, such an hypothesis can be reasonably discarded.

It can be concluded from these data that the conversion [$HCO_2H^{\bullet+}$, H_2O] into [HO–C–OH$^{\bullet+}$, H_2O] may occur within the complexes, but that the rate of dissociation by simple cleavage of the [HO–C–OH$^{\bullet+}$, H_2O] is much slower than other reactions such as protonation of water and decarbonylation.

The reason for the discrepancy in the reactions with water of ionized formamide and **FA**$^{\bullet+}$, lies in the reaction rate for proton transfer and decarbonylation which, in the case of **FA**$^{\bullet+}$ and **HyC**$^{\bullet+}$, proceed at near collision rate, in sharp contrast with the case of ionized formamide and of its carbene isomer where the reaction efficiency is only 4% [14]. This conclusion is confirmed by calculation.

4.2. Potential energy surface for the water catalyzed isomerization of *FA*$^{\bullet+}$ into *HyC*$^{\bullet+}$ and their decarbonylation

In order to precise the various steps of the decarbonylation reaction and of the competition between the protonation pathway and the isomerization pathway, an ab initio calculation of the potential energy surface (PES) was performed. Some elements of the potential energy surface for the $H_4CO_3^{\bullet+}$ system had already been calculated by other groups, at the B3LYP/6-31G** level by Hrùsak et al. [20]. This latter work does not provide a complete picture of the PES required to describe the system under study, since it did not take into account the decarbonylation pathway. Some key transition states for H atom loss and for proton transport isomerization were also not located in this previous work. These results have been completed by adding necessary points and by reoptimization of the already known geometries at the same UMP2/6-31G** level of the theory.

Table 1
G3(MP2) energies for the various stable conformers of **FA**$^{\bullet+}$ and **HyC**$^{\bullet+}$ (in kcal mol^{-1}, relative to the most stable conformer of **FA**$^{\bullet+}$)

Structure	E°_{298K}
FAa$^{\bullet+}$	0.0
FAb$^{\bullet+}$	0.5
HyCa$^{\bullet+}$	−9.5
HyCb$^{\bullet+}$	−5.8
HyCc$^{\bullet+}$	2.0

4.2.1. Various conformers can interconvert through a common intermediate

The number of conformers for the various structures under study complicates the study. For instance, **FA**$^{\bullet+}$ can have two stable conformers and **HyC**$^{\bullet+}$ three stable conformers (Table 1, Fig. 2). The strong steric interactions in **HyCc**$^{\bullet+}$ explain the destabilization of this ion compared to the two other conformers. Each of these can lead to a series of complexes with water. Fortunately the stabilities of these conformers are close from each others and the transition states linking these conformers lie below the transition states linking chemically different structures. Therefore calculation of all the possible structures was not necessary. For instance, three conformers of the proton bound dimer [HOCO$^{\bullet}\cdots H^+\cdots OH_2$] were located: **1a**, **1b**, **1c** (Table 2, Fig. 3). Some of the transition states that allow interconversion between these stable complexes were located (**TS1a/1b**, **TS1a/1c** and **TS1c/1c**). For this reason, although most of the stable conformers were computed, the search for transition states was limited to those linking the most stable conformers.

In coherence with the energy profile, when deuterium labeled compounds are used, some H/D scrambling can occur in the complex, through the transition state **TS1c/1c**. This agrees well with the experimental observations.

4.2.2. Water catalyzed isomerization between *FA*$^{\bullet+}$ and *HyC*$^{\bullet+}$

The water molecule can react with **FA**$^{\bullet+}$ to yield three types of complexes (Table 2, Fig. 4): a hydrogen bonded complex with the hydroxylic hydrogen of the acid (**2a** and

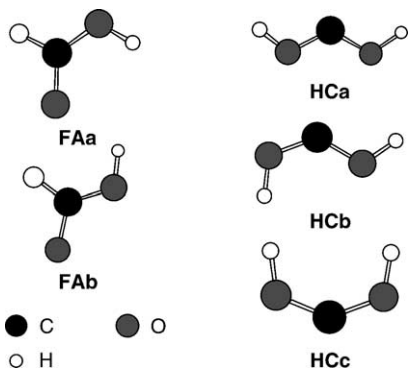

Fig. 2. Structures of the various conformers of **FA**$^{\bullet+}$ and **HyC**$^{\bullet+}$.

Table 2
G3(MP2) energies for the entry points, stable structures, exit points and transition states of the $\mathbf{FA}^{\bullet+}/\mathbf{HyC}^{\bullet+} + H_2O$ PES (in kcal mol^{-1}, relative to $\mathbf{FA}^{\bullet+} + H_2O$)

Structure	E°_{298K}	Structure	E°_{298K}	Structure	E°_{298K}
$\mathbf{FAa}^{\bullet+} + H_2O$	0.0	**6a**	−29.8	**TS1a/1b**	−32.4
$\mathbf{HyCa}^{\bullet+} + H_2O$	−9.5	**6b**	−27.9	**TS1a/1c**	−30.2
1a	−40.8	**7**	−19.0	**TS1c/1c**	−26.7
1b	−39.1	**8** + H$^{\bullet}$	−28.4	**TS1b/2a**	−0.2
1c	−37.5	$H_3O^+ + CO + OH^{\bullet}$	11.6	**TS1c/3**	−21.6
2a	−28.8	$[H_2O\cdots OH_2]^{\bullet+} + CO$	3.1	**TS1c/5b**	−24.7
2b	−28.3	$H_3O^+ + CHO_2^{\bullet}$	2.7	**TS1a/6a**	−30.4
3	−18.1	$H_2OH^+\cdots CO + OH^{\bullet}$	−2.3	**TS1c/8**	−3.8
4	−15.1	$[H_2OH^+\cdots OH^{\bullet}] + CO$	−9.3	**TS2a/4**	−14.5
5a	−24.2	$H_3O^+ + OCOH^{\bullet}$(b)	−10.9	**TS2a/8**	−18.0
5b	−21.2	$H_3O^+ + OCOH^{\bullet}$(a)	−12.7	**TS3/4**	−15.1
5c	−16.0	$H_3O^+ + CO_2 + H^{\bullet}$	−14.3	**TS6a/7**	−15.7

2b), a much less stable hydrogen bonded complex with the hydrogen borne by the carbon atom (**3**) or an electrostatic bonded complex (**4**). At the UMP2/6-31G** a transition state (**TS1c/3**) was located 0.9 kcal mol^{-1} above **3**. An IRC calculation was carried on to confirm the nature of this transition state. Therefore **3** readily evolves toward the H-bonded complex **1c**. This is formally an isomerization of a [$\mathbf{FA}^{\bullet+}$, H_2O] complex into a [$\mathbf{HyC}^{\bullet+}$, H_2O] complex, involving a catalyzed 1,2-H transport. As previously discussed for the conversion by water of ionized methanol into its α-distonic counterpart [12], the barrier for catalyzed isomerization is almost non-existent, as the water molecule tends to abstract the proton as soon as it reaches close enough to the hydrogen in **3**. This is even more obvious when searching for the conformer of **3** arising from $\mathbf{FAb}^{\bullet+}$: there is no minimum on the PES when following the O(H_2)–H(COOH$^{\bullet+}$) distance. The water molecule simply picks up the proton and shifts towards the deep **1a** minimum. No intermediate proton-bound dimer is observed, most probably since, in the radical, the electron pair is involved in a π C=O bond.

Starting now from **2a**, this ion can isomerize into **1** through two different processes. On the one hand, a high energy spectator mechanism (through **TS2a/1b**) for which the barrier is only 0.2 kcal mol^{-1} under the energy of the reactant ion; this pathway can be ruled out. On the other hand, a rotation of the water molecule around the $\mathbf{FA}^{\bullet+}$ moiety,

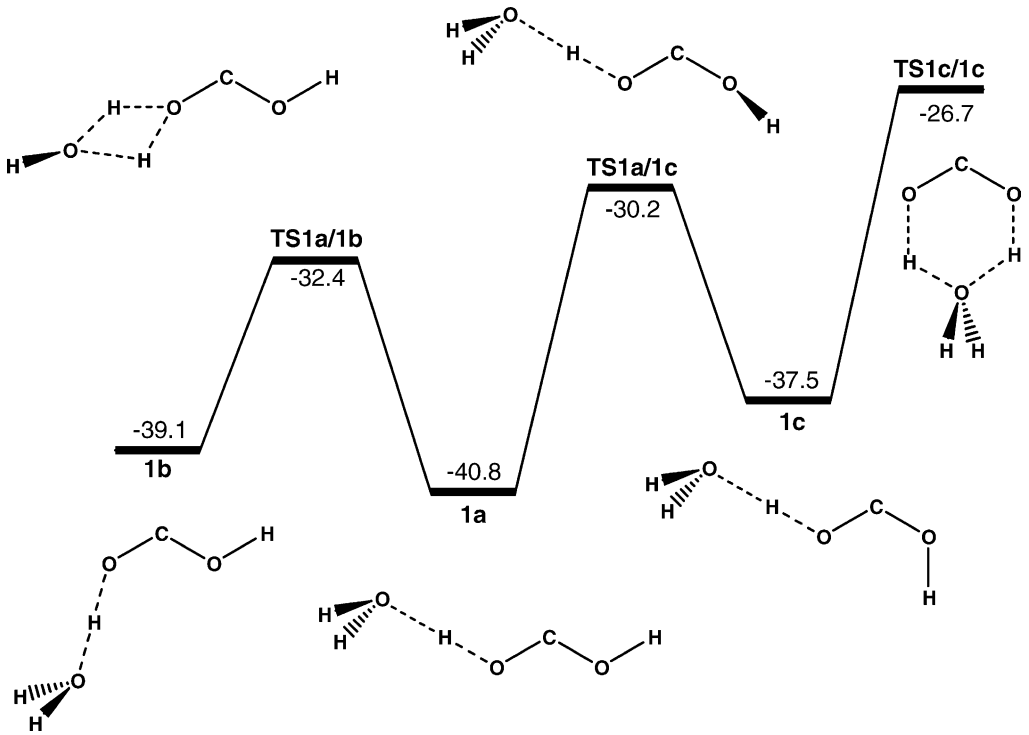

Fig. 3. Excerpt of the potential energy surface of the $\mathbf{FA}^{\bullet+} + H_2O$ system showing the barriers for interconversions between the [HOCO$^{\bullet}\cdots H^+\cdots OH_2$] conformers. E°_{298K} in kcal mol^{-1}, computed at the G3(MP2) level, relative to $\mathbf{FAa}^{\bullet+} + H_2O$.

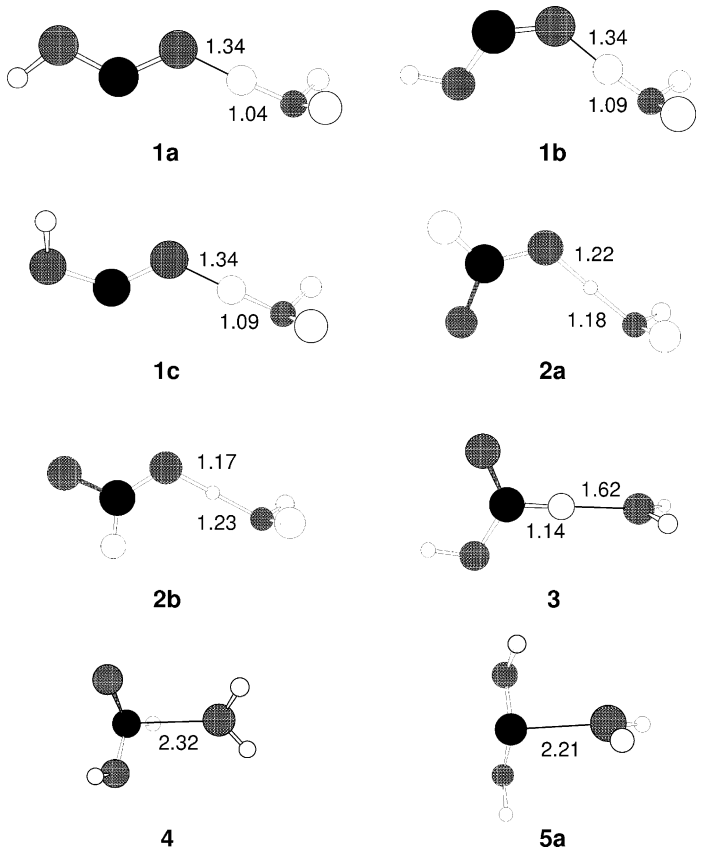

Fig. 4. Optimized structures of some significant complexes formed by the reaction of **FA**$^{\bullet+}$ or **HyC**$^{\bullet+}$ with water. Distances in Å, atom fillings are those of Fig. 2.

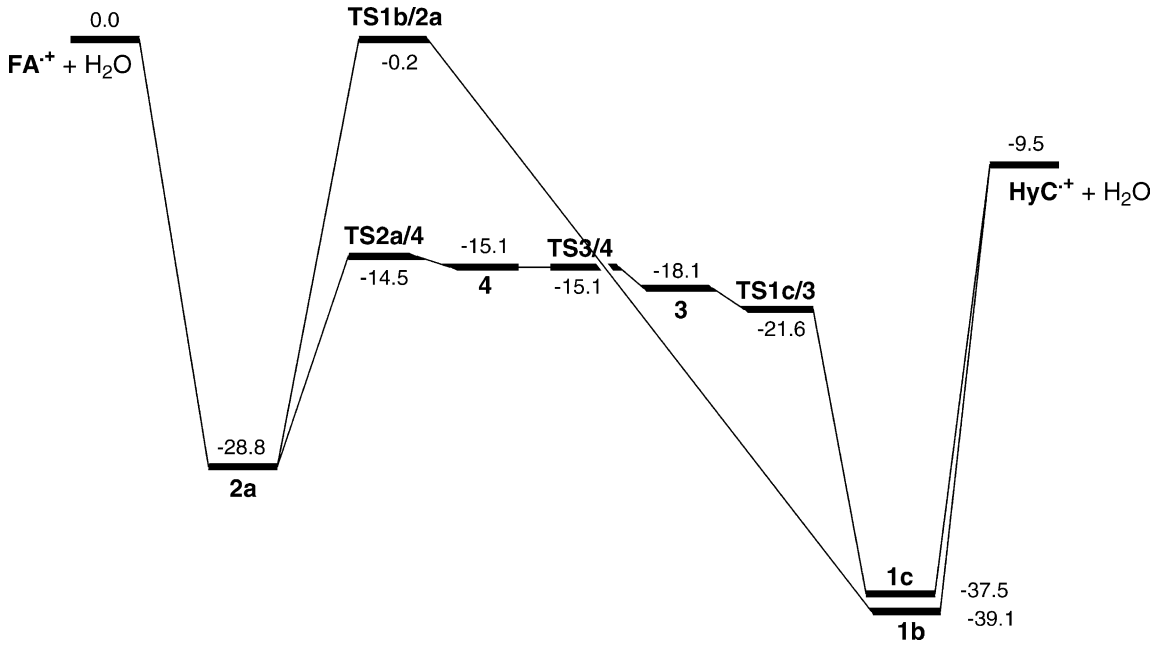

Fig. 5. Excerpt of the potential energy surface of the **FA**$^{\bullet+}$ + H_2O system showing the barriers for interconversions between **FA**$^{\bullet+}$ + H_2O and **HyC**$^{\bullet+}$ + H_2O. E°_{298K} in kcal mol^{-1}, computed at the G3(MP2) level, relative to **FAa**$^{\bullet+}$ + H_2O.

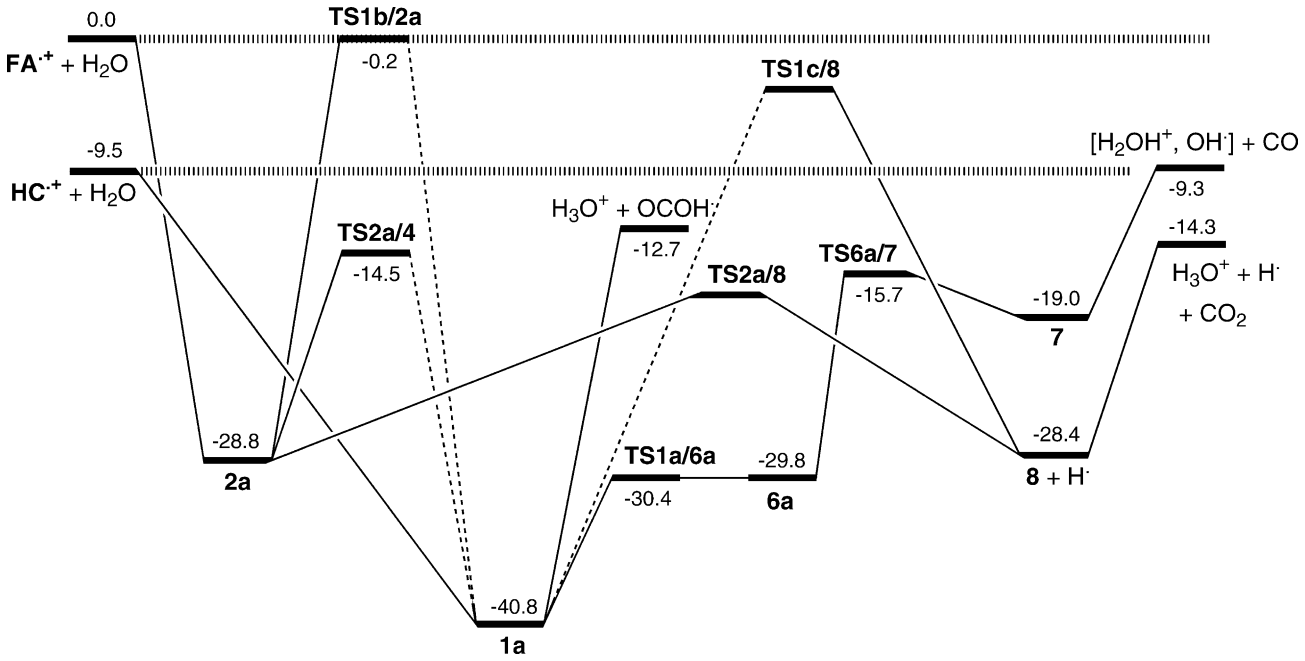

Fig. 6. Simplified PES of the $\mathbf{FA}^{\bullet+}/\mathbf{HyC}^{\bullet+} + H_2O$ system. E°_{298K} in kcal mol^{-1}, computed at the G3(MP2) level, relative to $\mathbf{FAa}^{\bullet+} + H_2O$. Full lines connecting states indicate direct connection; dashed lines indicate that only the most energetic transition state along the pathway has been shown for clarity. Hashed lines indicate the exothermicity limit for both $\mathbf{FAa}^{\bullet+} + H_2O$ and $\mathbf{HyCa}^{\bullet+} + H_2O$ systems.

through **TS2a/4** gives **4** and then through **TS3/4** leads to **3** (Fig. 5). Although much more steps are required, the highest barrier for this process lies 14.5 kcal mol^{-1} under the reactant energy. Therefore the real barrier in the process is the energy required to break the hydrogen bond in **2a** and bring the water molecule close to this very acidic hydrogen.

In conclusion, calculation confirms experiment: water solvated $\mathbf{FA}^{\bullet+}$ and water solvated $\mathbf{HyC}^{\bullet+}$ easily interconvert.

4.2.3. Lack of symmetrisation of the oxygen atoms

The key points of the potential energy surface are summarized in Fig. 6: only the most stable conformers are represented, and transition states mentioned are the limiting transition states when multiple transition states separate two stable species. The corresponding structures are in Figs. 4 and 7. It is worth noticing that, as already pointed out [14,15,19], there is no covalent addition of the water

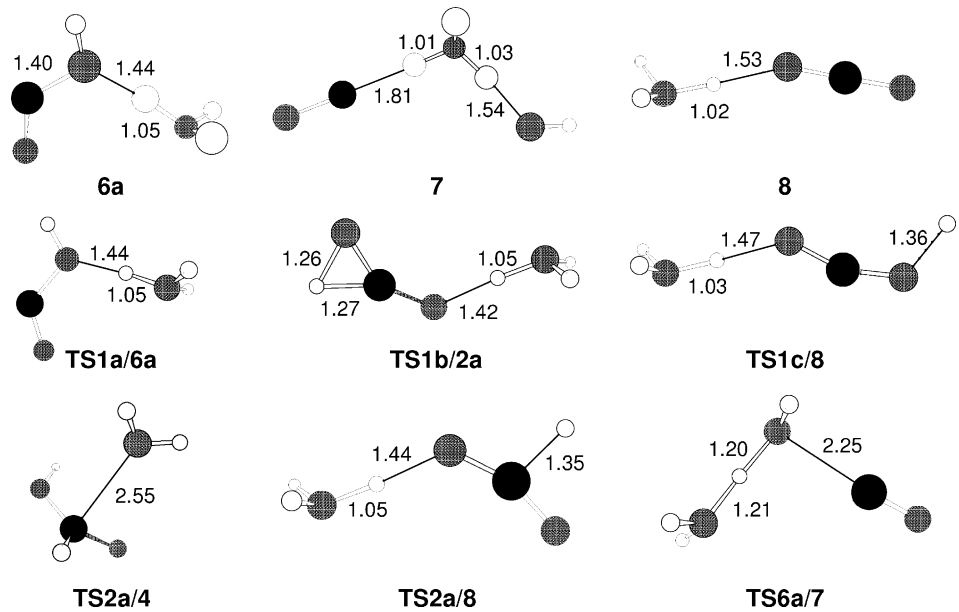

Fig. 7. Optimized structures of important complexes and transition states occurring in the reaction of $\mathbf{FA}^{\bullet+}$ or $\mathbf{HyC}^{\bullet+}$ with water. Distances in Å, atom fillings are those of Fig. 2.

molecule to the carbene. The only stable structures are electrostatically bound structures such as **5a** (Fig. 4), which can only evolve towards the group **1** ions. Therefore no symmetrization of the three oxygen atom can occur through H transfers in an intermediate distonic ion, which is in agreement with the products formed when the reactions are performed with $H_2{}^{18}O$.

4.2.4. Mechanisms for the formation of the $[H_2OH^+\cdots OH^\bullet]$ dimer

As shown by the experimental results, formation of the $[H_2O\cdots OH_2]^{\bullet+}$ dimer should be ruled out. Theoretical calculations confirm this result, as formation of this dimer would be endothermic by 3.1 kcal mol^{-1} starting from $\mathbf{FA}^{\bullet+} + H_2O$ (and 12.6 kcal mol^{-1} from the other isomer).

Formation of the $[H_2OH^+\cdots OH^\bullet]$ dimer proceeds in two steps from **1a**: the H_3O^+ moiety turns around the $OCOH^\bullet$ radical through a very low transition state leading to proton bound dimer $[H_2O\cdots H^+\cdots O(H)CO]$ **6a**. **TS1a/6a** connects these two minima of the PES, with a very early transition state as checked by an IRC calculation. This is not surprising considering that H_3O^+ migration is easy.

The transition state leading to the terbody complex **7** is intriguing: the net result of the reaction is the insertion of H_3O^+ in the C–OH bond of the $OCOH^\bullet$ radical. But the transition state **TS6a/7** looks more like a transition state for a proton transfer than that of an insertion, and IRC calculation confirms that it indeed connects **6a** and **7**. A plot of the distance of the bounding hydrogen versus the elongation of the C–OH bond (Fig. 8) leads to a surprising result: the proton is in fact transferred twice in a single reaction step. When increasing the C–O distance, it first moves from the water molecule to the other oxygen atom, leading to an $OC–OH_2{}^{\bullet+}$ radical solvated by a water molecule. This structure is not associated with a minimum on the PES but this transfer allows the elongation of the C–O bond: calculation on the non solvated $OCOH_2{}^{\bullet+}$ radical cation (7.3 kcal mol^{-1} less stable than $\mathbf{FAa}^{\bullet+}$) shows a very elongated C–O bond of 1.65 Å (Scheme 4). The atom in molecule (AIM) analysis

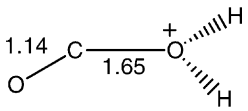

Scheme 4.

of this bond, based on the calculation of the Laplacian of the density function [32], shows a nearly null value at the midpoint of this bond, which is typical of non-covalent bond.

In a second time, the original water molecule recaptures the proton from the nearby $OH^\bullet$ moiety leading to the terbody complex, at first with an $OC\cdots OH^\bullet\cdots HOH_2{}^+$ structure, which evolves without any energy barrier to structure **7**. The transition state is situated at the point of the second proton transfer. The absence of any mixing of the oxygen atoms in the experiments with $H_2{}^{18}O$ supports this mechanism: the labeled oxygen is always located on the H_3O^+ moiety, and not the $OH^\bullet$ moiety, at the end of the reaction. Therefore, there does not exist any intermediate of the $[CO, H_2O, H_2O]^+$ structure with sufficient lifetime for the water molecule exchange to take place. Such a mechanism explains this by a strong localization of the charge on one migrating proton.

This terbody complex can then dissociate through loss of CO leading to the $[H_2OH^+\cdots OH^\bullet]$ dimer.

Formation of the $[H_3O^+\cdots CO]$ dimer is energetically feasible starting from the $\mathbf{FA}^{\bullet+}$ isomer. But this product is not observed, since $OH^\bullet$ loss would occur from **7** and since CO loss from this complex leads to a product 7 kcal mol^{-1} more stable.

4.2.5. Mechanisms for the formation of H_3O^+

Several mechanisms can a priori contribute to the formation of H_3O^+

(i) A first source is the exothermic direct protonation of water (from **3**) or from **1a**, **1b** or **1c** directly from $\mathbf{HyC}^{\bullet+}$ or after isomerization of $\mathbf{FA}^{\bullet+}$ into $\mathbf{HyC}^{\bullet+}$.
(ii) A second source is direct protonation by the carbon bound hydrogen of $\mathbf{FA}^{\bullet+}$ while direct protonation from

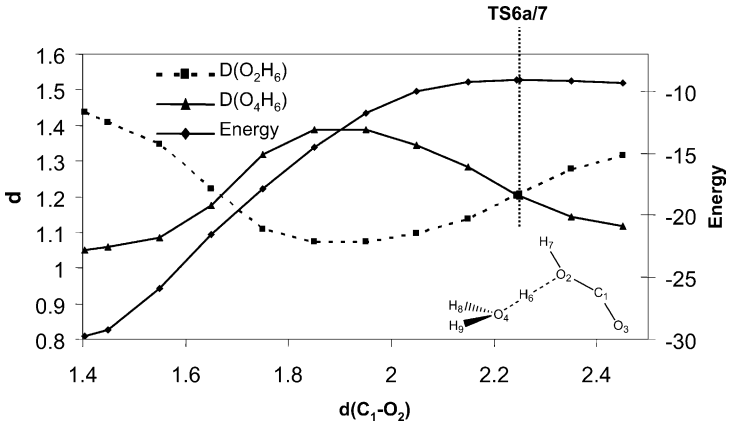

Fig. 8. Plot of the energy and of the O_2–H_6 and O_4–H_6 distances as a function of the C_1–O_2 distance in the approach of the transition state **TS6a/7**. Distances in Å, energies in kcal mol^{-1}.

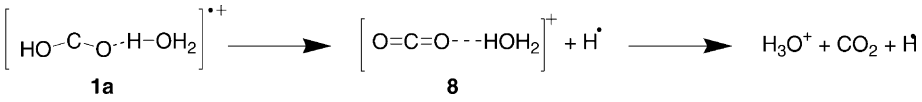

Scheme 5.

the hydroxylic hydrogen of **FA**$^{\bullet+}$ (from **2a** or **2b**) would be endothermic and therefore cannot occur.

Another pathway exists, involving the carbon bound hydrogen of **FA**$^{\bullet+}$, that also leads to the formation of an H_3O^+ ion, through a successive loss of H$^\bullet$ and CO_2 (Scheme 5). This pathway leads to the most exothermic exit points of the PES. It was described by the experimental results of Hrùsak et al. [20] although the transition states for the H$^\bullet$ loss were not located. This work was concerned with the dissociation of a $CO_3H_4^{\bullet+}$ ion formed by dissociation of ionized dihydroxyfumaric acid. The metastable dissociation leads mainly to H$^\bullet$ loss (98%) and to a small H_3O^+ peak. These results are in agreement with the PES calculated in this work: starting from **2a**, the loss of H$^\bullet$ can occur through a low **TS2a/8**, which lies only 10 kcal mol^{-1} above **2a**. Starting from **1a**, the direct loss of H$^\bullet$ requires 37 kcal mol^{-1} through **TS1c/8**. This transition state is above the dissociation to H_3O^+, therefore loss of OCOH$^\bullet$ should be the dominant channel. But isomerization of **1** to **2a** is possible through **TS2a/3** which reduces the energy requirement to only 26.3 kcal mol^{-1}.

The question then becomes: why is the loss of H$^\bullet$ not observed in the case of the ion–molecule reaction? The internal energy content of the complexes formed by ion–molecule reaction is presumably higher than that of ions selected in the metastable time-frame. Therefore, the [$H_2OH^+ \cdots$ OCO] complex **8** could be produced intermediately, but with sufficient energy to decompose into H_3O^+ in the ICR time frame.

5. Concluding remarks

A similar water catalyzed decarbonylation of ionized formamide and of its carbene isomer has been published previously [14]. It is of some interest to compare these two systems that behave in a similar way, in order to see what general trends on solvent catalyzed decarbonylation of ionized carbonyl compounds could be inferred from this set of results.

5.1. Catalysis of the keto-carbene isomerization

A first important similarity between these two cases is that the solvent molecule makes easy the interconversion between both isomers through a proton transport. The difference is that HCOOH$^{\bullet+}$ and $HCONH_2^{\bullet+}$ differ markedly in the acidity of the proton, or put, the other way around, in the proton affinities of the corresponding radicals (Scheme 6, values are computed at the G3(MP2) level for the $BH^+ + H_2O \rightarrow B + H_3O^+$ reaction, using the experimental PA(H_2O) = 165.2 kcal mol^{-1}). Ionized formamide is a ideal case for water catalyzed 1,2 proton transport: the proton affinity of the water molecule lies between that of the two basic sites of the radical. This transport is therefore easy according to the "PA rule" [9,12]. On the other hand, in the case of ionized formic acid, water is not an ideal catalyst since the PA of water lies 3.2 kcal mol^{-1} above that of the most basic site. As a consequence, the proton is never transferred back to the radical moiety: examination of the bond distances in the intermediate complexes **1** (Fig. 4) clearly show that the proton remains on the H_2O moiety. Search for structures where the proton was located on the OCOH$^\bullet$ radical did not lead to any stable structures.

The use of an appropriate catalyst with a proton affinity lower than that of water is a means to generate the carbene ion by the catalyzed 1,2 proton transport, as shown by the reaction of formic acid with CO and SO_2.

5.2. Catalyzed decarbonylation

The step preceding the loss of CO is very similar for both processes: in the case of ionized formamide it proceeds through a catalyzed 1,3 proton transport from the [$H_2NCOH^{\bullet+}$, H_2O] structure to a [$H_3NCO^{\bullet+}$, H_2O] structure. In the case of the ionized formic acid, there is no real proton transport since the proton remains attached to the water molecule, but the H bond shifts from one side of the radical to the other oxygen atom. It could still be formally

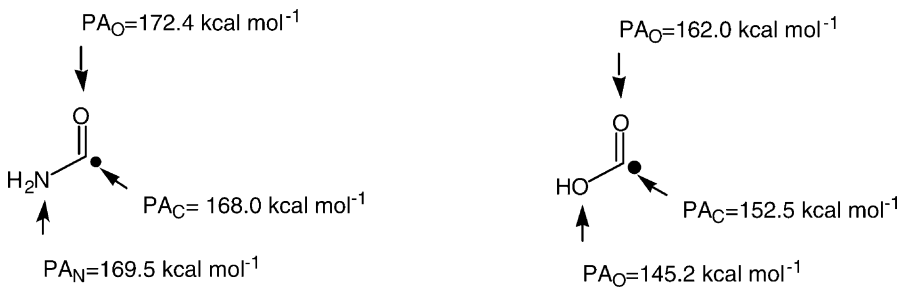

Scheme 6.

considered a 1,3 proton transport and remains similar to the previous case.

The elimination of CO seems different for both systems: in the ionized formamide system, simple elongation of the N–C bond in the [$H_3NCO^{\bullet+}$, H_2O] structure leads to the [NH_3, $H_2O]^{\bullet+}$ dimer. In the case of the ionized formic acid system, the process is complicated since the proton is not initially attached to the radical moiety. As discussed above, protonation of the $OCOH^{\bullet}$ radical leads to the elongation of the OC–OH_2 bond which can then dissociate as in the case of the $H_3NCO^{\bullet+}$ cation.

Although most steps are similar for both mechanisms, the final products differ: ionized formamide leads to the [NH_3, $H_2O]^{\bullet+}$ structure (and not [$H_3NH^+ \cdots OH^{\bullet}$]) whereas ionized formic acid leads to the [$H_2OH^+ \cdots OH^{\bullet}$] structure (and not [$H_2O$, $OH_2]^{\bullet+}$). One reason for this is simply that [$H_2OH^+ \cdots OH^{\bullet}$] is 12.8 kcal mol^{-1} more stable than its water dimer isomer (Fig. 5) which is therefore not accessible for the reaction. Another reason is that in the transition state **TS6a/7**, the proton is already shared between the $OH^{\bullet}$ radical and the H_2O molecule. In the similar transition state for the ionized formamide system, the proton is shared between an $NH_2^{\bullet}$ radical and the water molecule. The proton affinity of the $NH_2^{\bullet}$ radical (184.8 kcal mol^{-1}) being much higher than that of the $OH^{\bullet}$ radical (141.8 kcal mol^{-1}) [26], the proton remains on the ammonia molecule leading to the observed dimer.

In conclusion, the behavior of the $HCONH_2^{\bullet+}$/water system is very similar to that of $CH_3OH^{+\bullet}$/water system [12]. In both cases, a catalyzed 1,2-H transfer involving a very low energy barrier yields an isomerized product which can be isolated and characterized. In contrast, in the $HCOOH^{\bullet+}$/water system as well as in the $CH_3OH^{+\bullet}$ /methanol system [12], the 1,2-H transfer is catalyzed but the proton affinity of the catalyst is by far too high to permit the direct observation of the isomerized product. This kind of hidden isomerization may be widespread.

References

[1] (a) H. Becker, D. Schröder, W. Zummack, H. Schwarz, J. Am. Chem. Soc. 116 (1994) 1096;
(b) T. Weiske, H. Schwarz, Chem. Ber. 116 (1983) 323;
(c) T. Weiske, H. Halim, H. Schwarz, Chem. Ber. 118 (1985) 495;
(d) D. Schröder, J. Loos, M. Semialjac, T. Weiske, H. Schwarz, G. Höne, R. Thissen, O. Dutuit, Int. J. Mass Spectrom. 214 (2002) 105;
(e) J. Loos, D. Schröder, W. Zummack, H. Schwarz, R. Thissen, O. Dutuit, Int. J. Mass Spectrom. 214 (2002) 155, and references cited therein.

[2] S. Hammerum, Mass Spectrom. Rev. 7 (1988) 123.

[3] R.L. Smith, P.K. Chou, H.I. Kenttämaa, Structure and reactivity of selected distonic radical cations, in: T. Baer, C.-Y. Ng, I. Powis (Eds.), The Structure, Energetics and Dynamics of Organic Ions, John Wiley & Sons, Chichester, 1996, pp. 197–261.

[4] H.E Audier, J. Fossey, D. Leblanc, P. Mourgues, V. Troude, in: K.R. Jennings (Ed.), Intermediate in Ionic Gas Phase Chemistry II—Distonic Ions in Fundamental and Applications of Gas Phase Ion Chemistry, 1999, pp. 1–25.

[5] H.E. Audier, G. Sozzi, J.P. Denhez, Tetrahedron 42 (1986) 1179.

[6] G. Sozzi, H.E. Audier, A. Milliet, Bull. Soc. Chim. 11 (1984) 292.

[7] B.F. Yates, L. Radom, J. Am. Chem. Soc. 109 (1987) 2910.

[8] G. Bouchoux, N. Choret, Int. J. Mass Spectrom. 201 (2000) 161.

[9] M.J. McEvans, Flow tube studies of small isomeric ions, in: N.G. Adams, L.M. Blabcock (Eds.), Advances in Gas Phase Ion Chemistry, vol. 1, JAI Press, Greenwich, CT, 1992.

[10] D.K. Bohme, Int. J. Mass Spectrom. Ion Processes 115 (1992) 95.

[11] H.E. Audier, P. Mourgues, G. van der Rest, J. Chamot-Rooke, H. Nedev, Adv. Mass Spectrom. (2001) 101.

[12] (a) H.E. Audier, D. Leblanc, P. Mourgues, T.B. McMahon, S. Hammerum, J. Chem. Soc. Chem. Commun. (1994) 2329.;
(b) J.W. Gauld, L. Radom, J. Fossey, H.E. Audier, J. Am. Chem. Soc. 118 (1996) 6299;
(c) J.W. Gauld, L. Radom, J. Am. Chem. Soc. 119 (1997) 9831.

[13] (a) P.K. Chou, R.L. Smith, L.J. Chyall, H.I. Kenttämaa, J. Am. Chem. Soc. 117 (1995) 4374;
(b) H.E. Audier, J. Fossey, P. Mourgues, T.B. McMahon, S. Hammerum, J. Phys. Chem. 100 (1996) 18380;
(c) S.P. de Visser, L.J. de Koning, N.M.M. Nibbering, J. Am. Chem. Soc. 120 (1998) 1517;
(d) M.A. Trikoupis, D.J. Lavorato, J.K. Terlow, P.J.A. Ruttink, P.C. Burgers, Eur. Mass Spectrom. 5 (1999) 431.

[14] G. van der Rest, P. Mourgues, H. Nedev, H.E. Audier, J. Am. Chem. Soc. 124 (2002) 5561.

[15] J. Chamot-Rooke, P. Mourgues, G. van der Rest, H.E. Audier, Int. J. Mass Spectrom. 226 (2003) 249.

[16] (a) G. van der Rest, P. Mourgues, J. Tortajada, H.E. Audier, Int. J. Mass Spectrom. Ion Processes 179/180 (1998) 293;
(b) G. van der Rest, J. Chamot-Rooke, P. Mourgues, D. Leblanc, H.E. Audier, Book of Abstracts of the 14th International Mass Spectrometry Conference, Tampere (Finland), in: E.J. Karjalainen, A.E. Hesso, J.E. Jalonen, U.P. Karjalainen (Eds.), Helsinki, 1997, p. 185;
(c) M.A. Trikoupis, J.K. Terlow, P.C. Burgers, J. Am. Chem. Soc. 120 (1998) 12131;
(d) J. Chamot-Rooke, G. van der Rest, P. Mourgues, H.E. Audier, Int. J. Mass Spectrom. 195 (2000) 385;
(e) G. van der Rest, H. Nedev, J. Chamot-Rooke, P. Mourgues, T.B. McMahon, H.E. Audier, Int. J. Mass Spectrom. 202 (2000) 161;
(f) P. Mourgues, J. Chamot-Rooke, G. van der Rest, H. Nedev, H.E. Audier, T.B. McMahon, Int. J. Mass Spectrom. 210/211 (2001) 429;
(g) P. Mourgues, J. Chamot-Rooke, H. Nedev, H.E. Audier, J. Mass Spectrom. 36 (2001) 102;
(h) M.A. Trikoupis, P.C. Burgers, P.J.A. Ruttink, J.K. Terlouw, Int. J. Mass Spectrom. 210/211 (2001) 489.

[17] P.C. Burger, A. Mommers, J.L. Holmes, J. Am. Chem. Soc. 105 (1983) 5976.

[18] E. Uggerud, W. Koch, H. Schwarz, Int. J. Mass Spectrom. Ion Processes 73 (1986) 187.

[19] J. Hrusàk, G.A. Gibson, H. Schwarz, J.K. Terlouw, Int. J. Mass Spectrom. Ion Processes 160 (1997) 117.

[20] H.L. Sievers, H.F. Grützmacher, P. Caravatti, Int. J. Mass Spectrom. Ion Processes 157/158 (1996) 283.

[21] T. Su, W.J. Chesnavich, J. Chem. Phys. 76 (1982) 5183.

[22] P.C. Burgers, G.A. McGibbon, J.K. Terlouw, Chem. Phys. Lett. 224 (1994) 539.

[23] M.J. Frisch et al., Gaussian 98, Revision A.6, Gaussian Inc., Pittsburgh, PA (1998).

[24] A.P. Scott, L. Radom, J. Phys. Chem. 100 (1996) 16502.

[25] L.A. Curtiss, P.C. Redfern, K.J. Raghavachari, V. Rassoloo, J.A. Pople, J. Chem. Phys. 110 (1999) 4703.

[26] (a) S.G. Lias, J.E. Bartmess, J.F. Liebman, J.L. Holmes, R.D. Levin, W.G. Mallard, J. Phys. Chem. Ref. Data 17 (Suppl.) (1988) 1;
(b) E. Hunter, S.G. Lias, J. Phys. Chem. Ref. Data 27 (1998) 413.

[27] (a) M.A. Fender, Y.M. Sayed, F.T. Prochaska, J. Phys. Chem. 95 (1991) 2811;
(b) D. Laakso, P. Marshall, J. Phys. Chem. 96 (1992) 2471.

[28] (a) C.Y. Ng, D.J. Trevor, P.W. Tiedemann, S.T. Ceyer, P.L. Kronebusch, B.H. Mahan, Y.T. Lee, J. Phys. Chem. 67 (1977) 4235;
(b) K. Norwood, A. Ali, C.Y. Ng, J. Phys. Chem. 95 (1991) 8029.
[29] (a) P.M.N. Gill, L. Radom, J. Am. Chem. Soc. 110 (1988) 4931;
(b) M. Sodupe, A. Oliva, J. Bertran, J. Am. Chem. Soc. 116 (1994) 8249.
[30] M. Speranza, Inorg. Chem. 35 (1996) 6140.
[31] (a) A. Heck, T. Drewello, L.J. de Koning, N.N.M. Nibbering, Int. J. Mass Spectrom. Ion Processes 100 (1990) 611;
(b) S.P. de Visser, L.J. de Koning, N.N.M. Nibbering, J. Phys. Chem. 99 (1995) 15444.
[32] R.F.W. Bader, Atoms in Molecules. A Quantum Theory, Oxford University Press, Oxford, 1990.